ANNALES
UNIVERSITATIS MARIAE CURIE-SKŁODOWSKA
LUBLIN – POLONIA
VOL. LXX SECTIO AAA 2015

# CARBON AND OXYGEN ISOTOPE VARIABILITY AMONG FORAMINIFERA AND OSTRACOD CARBONATED SHELLS

François Fourel[a,*], François Martineau[a], Emoke Tóth[b], Agnes Görög[b], Gilles Escarguel[a] and Christophe Lécuyer[a, c]

[a] Laboratoire CNRS UMR 5125 "Paléoenvironnements & Paléobiosphère"
Université Lyon 1, Campus de la Doua, F-69622 Villeurbanne, France
[b] Department of Paleontology, University of Budapest
PO box 120, H-1518, Budapest, Hungary
[c] Institut Universitaire de France, 103 bd Saint-Michel, 75005 Paris, France
* corresponding author: François Fourel, Tel : +33 (0) 4 72 44 62 42
FAX : +33 (0) 4 72 43 35 88, email : Francois.Fourel@univ-lyon1.fr

ABSTRACT

This study investigates the effect of biological and environmental inter-individual variability on the meaning of $\delta^{18}O$ and $\delta^{13}C$ values acquired on small carbonated shells. First we present data obtained with a MultiPrep automated carbonate system on small sample sizes of a homogeneous carbonate material: Carrara marble. This demonstrates the capacities of the analytical system to reliably run small amounts of carbonates even down to 10 μg. Then we present two data sets obtained on real fossil samples of various size (*sensu* number of individual organisms) calibrated against the NBS19 carbonate standard. Both datasets evidence a clear trend of between-biological sample standard deviation increase for both $\delta^{18}O$ and $\delta^{13}C$ measurements when the number of pooled specimens per sample decreases. According to the results obtained from a systematic study of a geologically homogeneous sample of coeval fossil *Elphidium* foraminifera, we estimate that there is 95% of chances to reach between-biological sample standard deviation values higher than 1.02‰ ($\delta^{18}O$) and 1.45‰ $\delta^{13}C$) based on single-cell measurements. Such values are one order of magnitude higher than the instrumental standard deviations associated with these stable isotope ratios. Conversely, a minimum of 35 ($\delta^{18}O$) and 44 ($\delta^{13}C$) pooled specimens of *Elphidium* appears

necessary to reach a between-sample standard deviation ≤ 0.25‰ with a probability of 95%. Such biological intrinsic and irreducible variability between coeval individuals, and thus samples, clearly questions the interest for single-cell analyses, more precisely, for coastal marine species, such as *Elphidium,* subject to many environmental changes during their life-time. Indeed, strong variations in salinity or temperature, as well as biogenic fractionation, could influence the isotopic composition of an individual specimen. Results might be less problematic for an average community including several tests. This paper underlines uncertainties linked to specific environments in which selected organisms live, especially for paleoceanographic or paleoclimatic reconstruction purposes where secular oxygen and carbon isotope variations typically range from 0.5 to 1.5‰.

**Keywords:** stable isotope, foraminifera, ostracod, heterogeneity, single shell analysis

## 1. INTRODUCTION

Stable oxygen isotope measurements of carbonated fossil shells were the pioneering studies for determining the temperatures of past seawater (Urey, 1947; McCrea, 1950; Epstein et al., 1953). Many carbonate–secreting marine organisms are confined to marine platform settings. Such environments are highly influenced by continental runoff and coastal oceanic currents ultimately affecting, e.g., the depth gradients of temperature and salinity, and photocline and nutricline depths. Coccoliths constitute a large fraction of the oceanic nannoplankton since the Early Jurassic but their very small size (a few μm) still makes difficult the isotopic analysis of fossils at the species, or at least at the genus level (but see, e.g., Stoll and Ziveri, 2002; Stoll and Shimizu, 2009; Fink et al., 2010). Foraminifera are also unicellular organisms which size classically ranges from 40 μm up to ~1 mm; they appeared during the early Paleozoic but benthic and planktonic forms invaded the deep and surface oceans since the Cretaceous (Roth, 1989). The carbon and oxygen isotope compositions of their shells have been widely used to reconstruct marine paleoproductivity and paleotemperatures. For example, Shackleton (1967; 1986), Shackleton and Opdyke (1973) and Shackleton et al. (1983) revealed the existence of a first-order long-term cooling of Earth's surface since the Paleocene as well as the periodicity of the Quaternary glacial-interglacial stages. Huber et al. (1995; 2002), Schmidt and Mysak (1996) and Jenkyns et al. (2004) showed that the Cretaceous oceans about 100 My ago were much warmer than today, especially at high latitudes in the absence of permanent polar ice caps. The occurrence of foraminifera above and below the thermocline as well as from low to high latitudes led many researchers to use their stable isotope compositions, combined to Mg/Ca ratios, as proxies for both thermal structure of the oceans and volume of freshwater ice stored on the continents (e.g. Billups and Schrag, 2003; Lea et al., 2006 ).

For these large scales, in space (open ocean) and time (several hundred years resolution), measurements made on several species of the same aliquot seem to reflect the general (regional) conditions, within acceptable uncertainties for natural

environmental changes (van Sebille et al., 2014). The question of robustness and significance of the isotopic analysis is raised for a small amount of foraminifera, taken in specific areas (such as coastal areas) undertaking strong environmental variations.

In the past two decades, increase in the sensitivity of dual-inlet isotope ratio mass spectrometers and their coupling to automated on-line preparation devices allowed the analysis of very small amounts of calcium carbonate, down to the 5–10 μg level. This instrumental improvement opened the field of analysis of single carbonate-secreting unicellular organisms such as foraminifera with weights ranging from a few tenths to hundreds micrograms for most of them. Consequently, many workers established carbon and oxygen isotope seawater curves based on such single shell analysis techniques (e.g. Kelly et al., 1996; Price et al., 1998; Zachos et al., 2007). Nevertheless, inter-individual isotopic variability for both C and O has already been documented (Shuxi and Shackleton, 1990; Billups and Spero, 1995; Saraswati, 2004) and cannot be reduced only to analytical and instrumental accuracy. However, no convincing demonstration was made so far for identifying the environmental (temperature, $\delta^{18}O$ of water, productivity and $\delta^{13}C$ of DIC) and biological (physiology and phylogeny) drivers responsible for such isotopic differences between analyzed specimens. The knowledge of the amplitude of the inter-individual oxygen isotope variability is critical considering that most short- and long-term changes in the mean annual or seasonal temperature of surface waters that did not exceed 5°C against up to 15°C for deep waters during the Phanerozoic (e.g. Shackleton, 1986; Zachos et al., 2001; 2003; Pucéat et al., 2003; Joachimski et al., 2009). Indeed, the slope of the oxygen isotope fractionation equation between calcium carbonate and water is slightly higher than 4, hence corresponding to the temperature amplitude recorded by 1‰ change in the $\delta^{18}O$ value of any aquatic carbonated shell. On the other hand, short-term changes in productivity as well as long-term variations in oxidation or burial of sedimentary organic matter typically produce variations of ±3‰ in the carbon isotope composition of seawater (Schidlowski, 1987).

Consequently, the aim of this study is to explore the amplitude of both carbon and oxygen isotopic variability as a function of sample size (i.e., number of individual shells pooled in a sample). Selected targets were benthic foraminifera (*Elphidium* and *Ammonia*) and ostracods (*Aurila*) since they have been used for some paleoenvironmental reconstructions of aquatic environments (Holmes, 1996; Bauch et al., 2004). We are conscious that these species are not the most representative of large scale (in space and time) environmental reconstructions in paleoceanography. Although, as they are coastal species, strong environmental parameter changes are expected, and therefore, isotopic measurements performed on individual specimens could reflect strong range of variations.

# 2. MATERIAL AND METHODS

## 2.1. SAMPLE ORIGIN

The studied fossil samples come from the Sarmatian (Middle Miocene, 12.8-11.5 Ma) deposits of three boreholes (Perbál-5, Mány-17 and Mány-22) in the Zsámbék Basin, Hungary, which is located in the central part of the Pannonian Basin (Fig. 1 and 2). The lithology of the Sarmatian deposits is heterogeneous: clays, clay marls, calcareous marls, sandstones and limestones. The Sarmatian sequences are underlain by Badenian strata and overlain by Pannonian or Pleistocene sediments.


**Figure 1:** Geographical location of the studied fossils that were sampled from the Sarmatian (Middle Miocene, 12.8–11.5 Ma) deposits of three boreholes (Perbál-5, Mány-17 and Mány-22) in the Zsámbék Basin, Hungary.

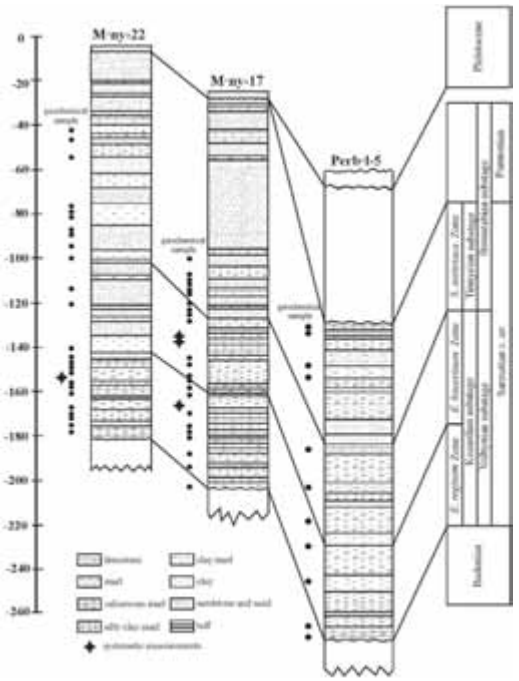


**Figure 2:** Lithostratigraphic Sarmatian successions in the three boreholes and location of foraminifera and ostracod samples.

For the analyses, very well preserved calcitic shells of foraminifera (*Elphidium aculeatum, E. macellum* and *Ammonia beccarii*) and ostracods (*Aurila mehesi* and *A. notata*) were selected (Fig. 3; see Görög (1992) and Tóth (2008) for detailed systematic descriptions of the studied species). The fossil shells are derived from 102 layers of the boreholes (Fig. 2, Appendix A). Additional specimens from four marly beds (Fig. 2, Appendix B) were collected for the systematic isotopic measurements.

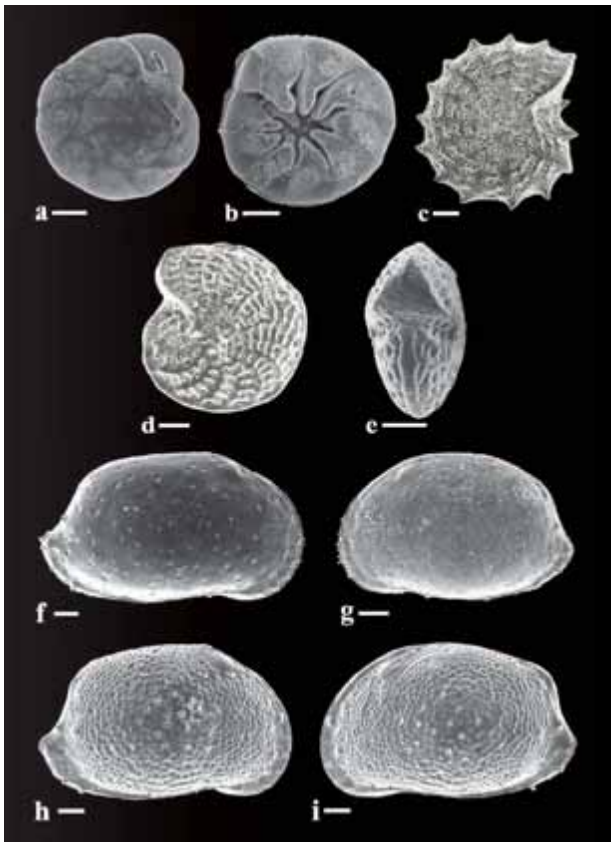


**Figure 3:** Foraminifera and ostracod species selected for stable carbon and oxygen isotope measurements. Scale bar=100 μm

(a) *Ammonia beccarii* (Linné). Dorsal side. Mány-22 borehole, depth 45-52.5 m.

(b) *Ammonia beccarii* (Linné). Ventral side. . Mány-22 borehole, depth 45-52.5 m.

(c) *Elphidium aculeatum* (d'Orbigny). Side view. Mány-17 borehole, depth 152.8-153 m.

(d) *Elphidium macellum* (Fichtel & Moll). Side view. Mány-22 borehole, depth 170-173 m.

(e) *Elphidium macellum* (Fichtel & Moll). Apertural view. Mány-22 borehole, depth 170-173 m.

(f) *Aurila mehesi* (Zalányi). RV. Mány-17 borehole, depth 168.7-171.2 m.

(g) *Aurila mehesi* (Zalányi). LV. Mány-17 borehole, depth 168.7-171.2 m.

(h) *Aurila notata* (Reuss). RV. Mány-22 borehole, depth 45-52.5 m.

(i) *Aurila notata* (Reuss). LV. Mány-22 borehole, depth 45-52.5 m.

### 2.2. SAMPLE TREATMENT

For each core sample and both C and O investigations, about 100 g of air-dried sediment was soaked in a dilute solution of hydrogen peroxide and then washed over a column of sieves of diminishing mesh sizes to extract the carbonated shells (foraminifera and ostracods). Then the shells were cleaned three times with deionized water in an ultrasonic bath to remove the sedimentary matrix, and finally hand-picked under a stereomicroscope. In all samples, the calcitic shells of foraminifera and ostracods preserved their original crystal structure as it was evidenced by X-ray diffraction data (Tóth et al., 2010), therefore precluding any diagenetic alteration of the pristine carbon and oxygen isotope compositions of the studied fossils.

### 2.3. ISOTOPE RATIO MEASUREMENT

Carbon and oxygen isotope ratio measurements have been performed with a MultiPrep system on line with a dual Inlet IsoPrime™ Isotope Ratio Mass Spectrometer (IRMS). The principle of the fully automated device is to react the calcium carbonates with anhydrous phosphoric acid at 90°C to generate $CO_2$ according to the following acid–base reaction:

$$CaCO_3 + H_3PO_4 \rightarrow CaHPO_4 + CO_2 + H_2O.$$

Each sample was carefully ground into a powder with grain sizes around 200 μm. Then the sample aliquot (typically 200 – 300 μg) was placed at the bottom of a V shape vial that was then sealed with a rubber septum. The sample vials were then placed in a temperature regulated sample tray heated at 90°C. From this stage all the sample preparation is done automatically. The MultiPrep system is equipped with a double hole needle which allows the acid to be delivered in the vial and also to extract the $CO_2$ which has been generated during the reaction. First the vial is evacuated through the external needle connected to the MultiPrep vacuum system. Then phosphoric acid is admitted in the vial through the inner needle using the acid pump. At this stage the reaction starts and $CO_2$ is generated. The reaction time is 20 min and during all this time the needle remains inside the valve. The external cold finger is maintained at -165°C and the valve arrangement allows the $CO_2$ generated from the reaction to be constantly extracted and trapped in the external cold finger. Once the reaction is completed the external cold finger is heated at -70°C to release the $CO_2$ without releasing water. The $CO_2$ pressure is read with a transducer located on the sample side of the IRMS Dual Inlet and from this pressure reading the sample analysis strategy is decided. If the sample is big enough it will be loaded in the dual inlet sample bellow and analyzed. If the sample is too small, it will be trapped in the Dual Inlet cold finger and analyzed.

# 3. RESULTS

## 3.1. BACKGROUND INSTRUMENTAL UNCERTAINTY

Determination of the instrumental noise is a prerequisite to any quantification of the carbon and oxygen isotopic variability between biological samples as a function of the number of analyzed individuals per sample. Therefore three sets of measurements have been performed on the international standard NBS–19 and an internal standard (Carrara Marble). Both were routinely measured on a daily basis over 2 months. Instrumental standard deviations associated with $\delta^{18}O$ and $\delta^{13}C$ measurements of "large" aliquots (~300 μg) of both NBS–19 and Carrara marble are of 0.062‰ and 0.022‰ (NBS–19, n=49) (Table 1; Figure 4), and of 0.069‰ and 0.036‰ (Carrara marble, n=30) (Table 2; Figure 5), respectively. These comparable results allow concluding that both calcium carbonate matrices have the same degree of isotopic homogeneity, and that the Carrara marble can be consequently used instead of NBS–19 in order to evaluate the standard deviations associated with measurements of natural samples of varying size.

**TABLE 1:** Carbon and oxygen isotope compositions of NBS19 aliquots over a period of six months. Sample weights vary from 280 to 390 μg. N.a.: not applicable (in case where only one measurement was performed).

| NBS-19-# | $\delta^{13}C$ ‰ V–PDB | S.D. | $\delta^{18}O$ ‰ V–PDB | S.D. |
|---|---|---|---|---|
| NBS19-1 | 1.93 | 0.004 | -2.33 | 0.011 |
| NBS19-2 | 1.96 | 0.026 | -2.16 | 0.185 |
| NBS19-3 | 1.96 | 0.081 | -2.16 | 0.239 |
| NBS19-4 | 1.94 | 0.024 | -2.26 | 0.100 |
| NBS19-5 | 1.94 | 0.027 | -2.15 | 0.222 |
| NBS19-6 | 1.96 | 0.023 | -2.23 | 0.041 |
| NBS19-7 | 1.92 | n.a. | -2.27 | n.a. |
| NBS19-8 | 1.98 | 0.042 | -2.14 | 0.092 |
| NBS19-9 | 1.93 | 0.016 | -2.22 | 0.058 |
| NBS19-10 | 1.96 | 0.017 | -2.15 | 0.094 |
| NBS19-11 | 1.93 | 0.007 | -2.30 | 0.027 |
| NBS19-12 | 1.95 | 0.022 | -2.23 | 0.050 |
| NBS19-13 | 1.97 | n.a. | -2.17 | n.a. |
| NBS19-14 | 1.98 | 0.011 | -2.12 | 0.013 |
| NBS19-15 | 1.91 | 0.006 | -2.18 | 0.131 |
| NBS19-16 | 1.93 | n.a. | -2.29 | n.a. |
| NBS19-17 | 1.98 | 0.032 | -2.12 | 0.125 |
| NBS19-18 | 1.96 | 0.058 | -2.22 | 0.081 |
| NBS19-19 | 1.94 | 0.027 | -2.17 | 0.134 |
| NBS19-20 | 1.93 | 0.003 | -2.33 | 0.017 |
| NBS19-21 | 1.96 | 0.027 | -2.15 | 0.068 |
| NBS19-22 | 1.96 | 0.000 | -2.12 | 0.046 |
| NBS19-23 | 1.94 | 0.011 | -2.24 | 0.019 |

Ctnd. **TAB. 1.**

| | | | | |
|---|---|---|---|---|
| NBS19-24 | 1.96 | 0.023 | -2.16 | 0.047 |
| NBS19-25 | 1.94 | 0.041 | -2.26 | 0.132 |
| NBS19-26 | 1.93 | 0.023 | -2.24 | 0.055 |
| NBS19-27 | 1.98 | 0.007 | -2.11 | 0.002 |
| NBS19-28 | 1.93 | 0.055 | -2.21 | 0.194 |
| NBS19-29 | 1.94 | 0.010 | -2.26 | 0.021 |
| NBS19-30 | 1.97 | 0.021 | -2.14 | 0.038 |
| NBS19-31 | 1.95 | 0.010 | -2.20 | 0.005 |
| NBS19-32 | 1.95 | 0.007 | -2.20 | 0.006 |
| NBS19-33 | 1.95 | n.a. | -2.20 | n.a. |
| NBS19-34 | 2.00 | 0.057 | -2.31 | 0.139 |
| NBS19-35 | 1.90 | 0.034 | -2.08 | 0.154 |
| NBS19-36 | 1.97 | 0.028 | -2.21 | 0.107 |
| NBS19-37 | 1.95 | 0.031 | -2.22 | 0.041 |
| NBS19-38 | 1.98 | 0.001 | -2.16 | 0.034 |
| NBS19-39 | 1.97 | 0.047 | -2.15 | 0.212 |
| NBS19-40 | 1.96 | 0.005 | -2.20 | 0.039 |
| NBS19-41 | 1.90 | 0.044 | -2.28 | 0.101 |
| NBS19-42 | 1.95 | 0.021 | -2.20 | 0.063 |
| NBS19-43 | 1.95 | 0.028 | -2.20 | 0.121 |
| NBS19-44 | 1.95 | 0.010 | -2.20 | 0.087 |
| NBS19-45 | 1.97 | 0.036 | -2.25 | 0.087 |
| NBS19-46 | 1.96 | 0.022 | -2.16 | 0.094 |
| NBS19-47 | 1.93 | 0.038 | -2.17 | 0.124 |
| NBS19-48 | 1.98 | 0.054 | -2.11 | 0.123 |
| NBS19-49 | 1.92 | 0.072 | -2.30 | 0.181 |

**TABLE 2:** Carbon and oxygen isotope compositions of Carrara marble aliquots over a period of six months. Sample weights vary from 100 to 350 μg.

| CM-# | $\delta^{13}C$ ‰ V–PDB | S.D. | $\delta^{18}O$ ‰ V–PDB | S.D. |
|---|---|---|---|---|
| CM1 | 1.993 | 0.044 | -1.762 | 0.061 |
| CM2 | 2.029 | 0.015 | -1.962 | 0.079 |
| CM3 | 2.082 | 0.017 | -1.819 | 0.006 |
| CM4 | 2.037 | 0.023 | -1.836 | 0.051 |
| CM5 | 2.054 | 0.072 | -1.758 | 0.194 |
| CM6 | 2.054 | 0.031 | -1.846 | 0.010 |
| CM7 | 1.987 | 0.023 | -1.975 | 0.068 |
| CM8 | 1.963 | 0.011 | -2.056 | 0.026 |
| CM9 | 1.987 | 0.032 | -1.968 | 0.109 |
| CM10 | 1.912 | 0.083 | -2.016 | 0.180 |
| CM12 | 1.944 | 0.044 | -1.796 | 0.061 |
| CM13 | 2.009 | 0.076 | -1.846 | 0.043 |
| CM14 | 1.997 | 0.080 | -1.828 | 0.029 |
| CM15 | 1.995 | 0.063 | -1.917 | 0.101 |
| CM16 | 2.067 | 0.024 | -1.826 | 0.110 |
| CM18 | 1.990 | 0.063 | -1.884 | 0.114 |
| CM20 | 2.043 | 0.037 | -1.880 | 0.045 |

Ctnd. **TAB. 2.**

| | | | | |
|---|---|---|---|---|
| CM21 | 1.958 | 0.061 | -1.865 | 0.088 |
| CM22 | 2.032 | 0.030 | -1.833 | 0.020 |
| CM23 | 2.018 | 0.032 | -1.849 | 0.052 |
| CM24 | 2.029 | 0.052 | -1.837 | 0.058 |
| CM25 | 2.019 | 0.026 | -1.848 | 0.085 |
| CM26 | 2.034 | 0.030 | -1.822 | 0.022 |
| CM27 | 2.016 | 0.026 | -1.861 | 0.021 |
| CM28 | 2.028 | 0.056 | -1.830 | 0.088 |
| CM29 | 2.022 | 0.019 | -1.853 | 0.053 |
| CM30 | 2.029 | 0.024 | -1.832 | 0.066 |
| CM31 | 2.020 | 0.022 | -1.852 | 0.044 |
| CM32 | 2.028 | 0.025 | -1.834 | 0.033 |
| CM33 | 2.021 | 0.010 | -1.851 | 0.027 |

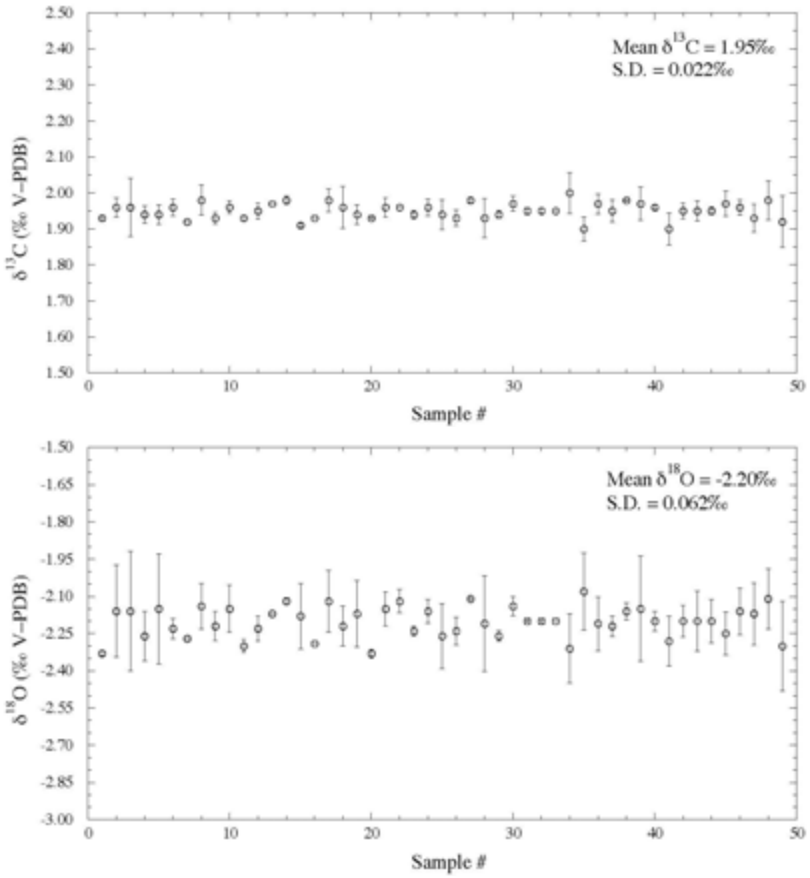


**Figure 4:** Evolution of $\delta^{13}C$ and $\delta^{18}O$ values of NBS 19 reference calcite over a period of six months. Sample sizes vary from 280 to 390 μg.

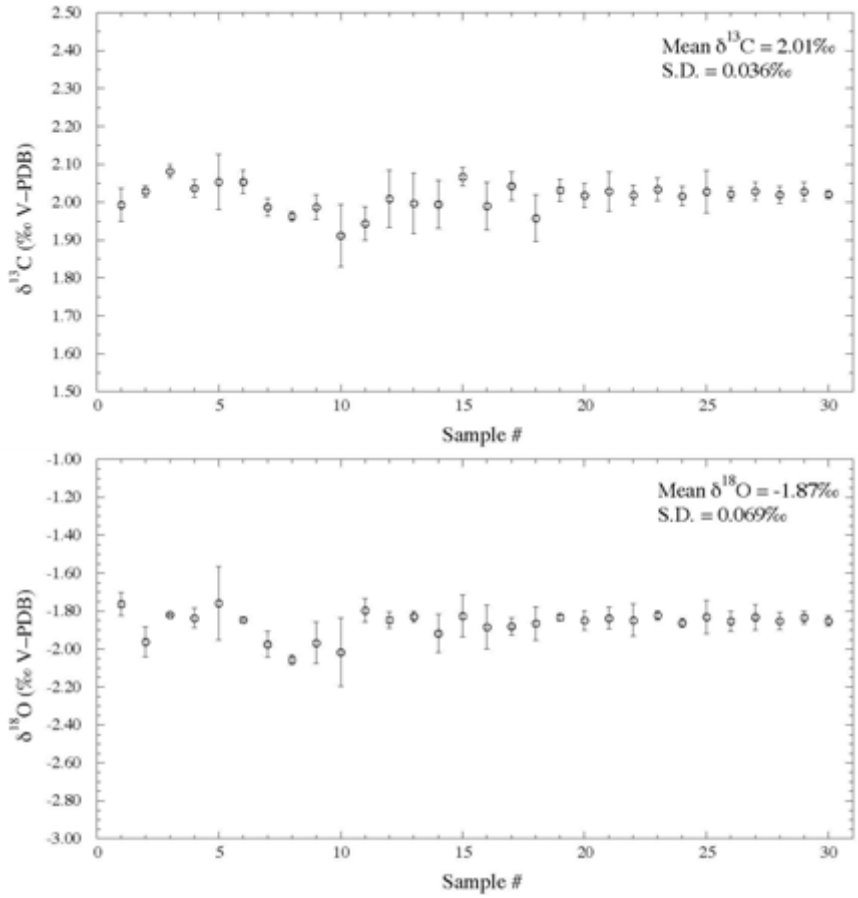


**Figure 5:** Evolution of $\delta^{13}C$ and $\delta^{18}O$ values of Carrara marble over a period of six months. Sample sizes vary from 100 to 350 μg.

Consequently, $\delta^{18}O$ and $\delta^{13}C$ standard deviations corresponding to the background instrumental noise have been further estimated for a series of Carrara marble aliquots of varying weight from 10 to 380 μg; the 29 performed measurements reveal that average instrumental standard deviations associated with $\delta^{18}O$ and $\delta^{13}C$ are of 0.133‰ and 0.057‰, respectively (Table 3; Figure 6). It is worth noting here that the average instrumental standard deviations estimated for aliquots ranging from 10 to 60 μg (0.155‰ for $\delta^{18}O$, and 0.067‰ for $\delta^{13}C$) were larger than those obtained for aliquots ranging from 110 to 380 μg (0.093‰ for $\delta^{18}O$ and 0.035‰ for $\delta^{13}C$), illustrating the expected increase in instrumental uncertainty with decreasing quantity of analyzed material (Fig. 6).

**TABLE 3:** Carbon and oxygen isotope compositions of Carrara marble aliquots which sample sizes range from 10 to 380 μg.

| Sample Name | Weight (μg) | $\delta^{13}C$ ‰ V–PDB | $\delta^{18}O$ ‰ V–PDB |
|---|---|---|---|
| CM8 | 10 | 1.99 | -1.90 |
| CM15 | 10 | 2.07 | -1.59 |
| CM22 | 10 | 2.10 | -1.58 |
| CM23 | 10 | 1.99 | -1.68 |
| CM27 | 10 | 1.99 | -1.64 |
| CM28 | 10 | 1.91 | -1.80 |
| CM29 | 10 | 1.98 | -1.56 |
| CM7 | 30 | 1.90 | -2.03 |
| CM24 | 30 | 1.95 | -1.76 |
| CM25 | 40 | 2.07 | -1.65 |
| CM26 | 60 | 1.92 | -1.88 |
| CM4 | 110 | 2.04 | -1.85 |
| CM5 | 110 | 2.05 | -1.80 |
| CM14 | 110 | 2.05 | -1.78 |
| CM19 | 140 | 2.02 | -1.85 |
| CM20 | 140 | 1.98 | -1.99 |
| CM21 | 150 | 2.02 | -1.93 |
| CM6 | 160 | 2.07 | -1.69 |
| CM13 | 170 | 2.05 | -1.86 |
| CM12 | 180 | 2.01 | -1.87 |
| CM3 | 210 | 2.04 | -1.96 |
| CM2 | 260 | 2.03 | -2.04 |
| CM10 | 270 | 2.10 | -1.82 |
| CM11 | 270 | 2.08 | -1.81 |
| CM16 | 280 | 2.12 | -1.71 |
| CM17 | 280 | 2.05 | -1.86 |
| CM1 | 290 | 2.01 | -1.99 |
| CM9 | 290 | 2.06 | -1.83 |
| CM18 | 380 | 2.09 | -1.84 |

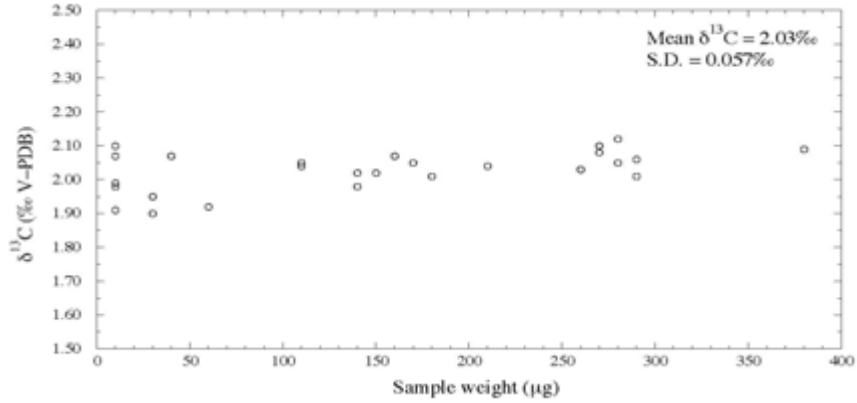

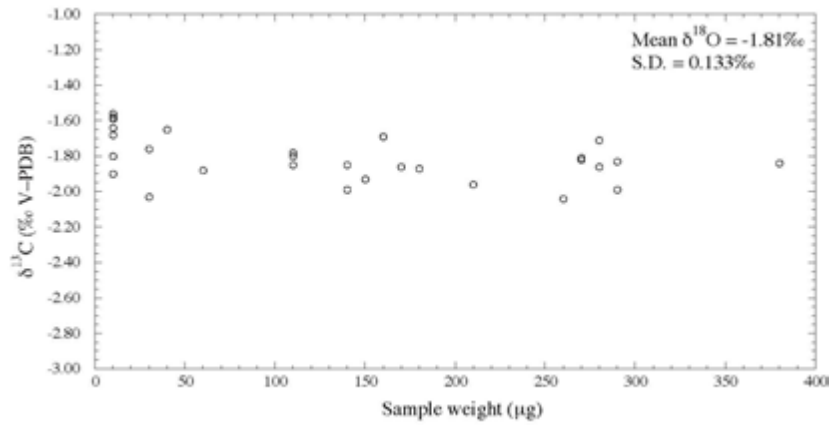


**Figure 6:** Variations in $\delta^{13}C$ and $\delta^{18}O$ values as a function of sample weights (10 to 380 µg) of Carrara marble.

## 3.2. INTER-INDIVIDUAL BIOLOGICAL VARIABILITY

Taking into account this background instrumental uncertainty, the following hypothesis was tested with natural microfossil samples of foraminifera (*Elphidium*; n=51 and *Ammonia*; n=16) and ostracods (*Aurila*; n=34): for a given sample weight, the between-biological sample isotopic variability should be independent on the number of individuals pooled in each analyzed sample. Table 4 and Figure 7 show that between-biological sample standard deviations related to $\delta^{18}O$ and $\delta^{13}C$ average empirical values increase up to 0.7‰ ($\delta^{18}O$) and 0.85‰ ($\delta^{13}C$) with the number of individuals decreasing; most values being larger than the background instrumental standard deviations. Data were non-linearly least–square fitted with a power law, assuming that the standard deviation tends towards infinite values when the number of individuals per sample tends towards zero, whilst it should tend towards the background instrumental noise, i.e. the standard deviation defined by either large samples of NBS–19 or Carrara marble, when the number of individuals per sample becomes very large.

**TABLE 4:** Carbon and oxygen isotope compositions of Sarmatian foraminifera (*Elphidium*, *Ammonia)* and ostracod (*Aurila)* samples. Standard deviations were calculated from two replicates of each sample.

| Sample # | Species | Weight (µg) | Individuals (n) | Mean $\delta^{13}C$ ‰ V–PDB | S.D. | Mean $\delta^{18}O$ ‰ V–PDB | S.D. |
|---|---|---|---|---|---|---|---|
| PB-5-1 | *Elphidium aculeatum* | 300 | 10 | -1.00 | 0.078 | -1.07 | 0.018 |
| PB-5-4 | *Elphidium macellum* | 300 | 15 | -0.98 | 0.055 | -1.69 | 0.108 |
| PB-5-5 | *Elphidium macellum* | 290 | 14 | 0.39 | 0.252 | -1.25 | 0.147 |
| PB-5-7 | *Elphidium aculeatum* | 300 | 9 | 0.73 | 0.111 | 0.25 | 0.160 |

ctnd. **TAB. 4.**

| | | | | | | | |
|---|---|---|---|---|---|---|---|
| PB-5-8 | *Elphidium macellum* | 310 | 12 | 0.04 | 0.102 | 0.20 | 0.182 |
| PB-5-17 | *Elphidium macellum* | 310 | 15 | 0.55 | 0.004 | -0.52 | 0.150 |
| PB-5-20 | *Elphidium macellum* | 300 | 8 | 0.77 | 0.111 | -2.93 | 0.164 |
| PB-5-21 | *Elphidium macellum* | 310 | 5 | 0.91 | 0.443 | -2.53 | 0.005 |
| PB-5-23 | *Elphidium macellum* | 310 | 14 | 1.10 | 0.069 | -2.93 | 0.217 |
| PB-5-25 | *Elphidium macellum* | 310 | 14 | 1.29 | 0.055 | -2.35 | 0.038 |
| PB-5-26 | *Elphidium macellum* | 310 | 6 | 0.55 | 0.260 | -2.30 | 0.036 |
| PB-5-28 | *Elphidium aculeatum* | 320 | 13 | 0.58 | 0.096 | -2.34 | 0.083 |
| PB-5-29 | *Elphidium macellum* | 310 | 7 | 1.54 | 0.040 | -2.13 | 0.081 |
| PB-5-33 | *Elphidium macellum* | 300 | 9 | 1.50 | 0.079 | -1.68 | 0.287 |
| PB-5-34 | *Elphidium aculeatum* | 310 | 5 | 1.80 | 0.040 | -0.45 | 0.025 |
| PB-5-36 | *Elphidium macellum* | 300 | 12 | 1.82 | 0.005 | -1.73 | 0.137 |
| PB-5-38 | *Elphidium aculeatum* | 310 | 16 | 0.48 | 0.073 | -0.13 | 0.170 |
| PB-5-46 | *Elphidium hauerinum* | 280 | 41 | -0.16 | 0.021 | -0.77 | 0.061 |
| PB-5-47 | *Elphidium macellum* | 310 | 26 | -0.69 | n.a. | -1.92 | 0.021 |
| PB-5-48 | *Elphidium macellum* | 280 | 35 | -0.55 | 0.064 | -1.87 | 0.031 |
| PB-5-50 | *Elphidium macellum* | 310 | 18 | -0.62 | 0.082 | -2.58 | 0.102 |
| PB-5-51 | *Elphidium macellum* | 300 | 25 | -0.36 | 0.107 | -1.59 | 0.197 |
| PB-5-53 | *Elphidium macellum* | 300 | 26 | 0.13 | 0.123 | -1.35 | 0.010 |
| PB-5-54 | *Elphidium macellum* | 300 | 24 | 0.88 | 0.060 | -1.62 | 0.184 |
| PB-5-57 | *Elphidium macellum* | 290 | 33 | -0.20 | 0.004 | -0.53 | 0.116 |
| M-17-2 | *Elphidium macellum* | 310 | 21 | 0.75 | 0.027 | -2.47 | 0.137 |
| M-17-4 | *Elphidium macellum* | 310 | 17 | 0.59 | 0.322 | -1.00 | 0.052 |
| M-17-6 | *Elphidium aculeatum* | 330 | 7 | 1.35 | 0.140 | -1.43 | 0.125 |
| M-17-8 | *Elphidium aculeatum* | 310 | 10 | 2.45 | 0.429 | -1.00 | 0.122 |

ctnd. **TAB. 4.**

| | | | | | | | |
|---|---|---|---|---|---|---|---|
| M-17-11 | *Elphidium macellum* | 320 | 18 | 1.53 | 0.072 | -1.09 | 0.108 |
| M-17-13 | *Elphidium aculeatum* | 330 | 14 | 1.13 | 0.134 | -0.59 | 0.178 |
| M-17-14 | *Elphidium aculeatum* | 330 | 13 | 0.88 | 0.043 | -0.73 | 0.394 |
| M-17-16 | *Elphidium macellum* | 310 | 46 | -0.08 | 0.029 | -1.09 | 0.091 |
| M-17-18 | *Elphidium macellum* | 310 | 21 | 1.38 | 0.263 | -1.52 | 0.029 |
| M-17-20 | *Elphidium macellum* | 310 | 12 | -0.37 | 0.296 | -1.20 | 0.136 |
| M-17-22 | *Elphidium macellum* | 300 | 14 | 0.27 | 0.097 | -2.22 | 0.037 |
| M-17-24 | *Elphidium macellum* | 290 | 16 | -0.59 | 0.027 | -1.32 | 0.042 |
| M-17-25 | *Elphidium macellum* | 320 | 27 | -0.09 | 0.005 | -2.24 | 0.277 |
| M-17-26 | *Elphidium macellum* | 320 | 21 | -0.40 | 0.039 | -1.70 | 0.191 |
| M-17-29 | *Elphidium macellum* | 320 | 10 | 1.08 | 0.034 | -1.46 | 0.139 |
| M-17-30 | *Elphidium macellum* | 290 | 27 | 0.38 | 0.043 | -0.84 | 0.080 |
| M-17-31 | *Elphidium aculeatum* | 300 | 21 | -0.12 | 0.073 | -1.13 | 0.068 |
| M-17-32 | *Elphidium macellum* | 300 | 21 | 0.98 | 0.101 | -1.48 | 0.147 |
| M-17-34 | *Elphidium macellum* | 310 | 17 | 1.30 | 0.475 | -3.21 | 0.090 |
| M-17-36 | *Elphidium macellum* | 300 | 8 | 1.86 | 0.092 | -2.83 | 0.070 |
| M-17-37 | *Elphidium macellum* | 310 | 14 | -0.98 | 0.145 | -1.18 | 0.032 |
| M-17-38 | *Elphidium macellum* | 290 | 11 | 1.92 | 0.006 | -1.19 | 0.124 |
| M-17-40 | *Elphidium macellum* | 290 | 13 | 0.58 | 0.210 | -2.28 | 0.423 |
| M-17-42 | *Elphidium macellum* | 310 | 10 | 1.04 | 0.316 | -2.52 | 0.055 |
| M-17-44 | *Elphidium macellum* | 310 | 13 | 1.11 | 0.229 | -2.18 | 0.066 |
| M-17-46 | *Elphidium macellum* | 320 | 28 | 0.49 | 0.348 | -1.74 | 0.689 |
| PB-5-6 | *Ammonia becarii* | 240 | 35 | -0.72 | 0.167 | -2.15 | 0.178 |
| PB-5-11 | *Ammonia becarii* | 210 | 25 | -0.09 | 0.003 | -1.08 | 0.183 |
| PB-5-13 | *Ammonia becarii* | 350 | 14 | 0.65 | 0.003 | -2.49 | 0.190 |

ctnd. **TAB. 4.**

| | | | | | | | |
|---|---|---|---|---|---|---|---|
| PB-5-16 | *Ammonia becarii* | 320 | 1 | 0.36 | 0.099 | -2.20 | 0.293 |
| PB-5-31 | *Ammonia becarii* | 310 | 19 | 0.91 | 0.062 | -2.90 | 0.108 |
| PB-5-37 | *Ammonia becarii* | 290 | 25 | 0.67 | 0.072 | -1.98 | 0.077 |
| PB-5-42 | *Ammonia becarii* | 300 | 28 | -0.13 | 0.071 | -2.77 | 0.201 |
| PB-5-43 | *Ammonia becarii* | 290 | 36 | -0.33 | 0.084 | -2.15 | 0.081 |
| PB-5-44 | *Ammonia becarii* | 300 | 41 | 0.93 | 0.089 | -2.05 | 0.115 |
| PB-5-45 | *Ammonia becarii* | 300 | 44 | -0.84 | 0.100 | -1.09 | 0.051 |
| PB-5-49 | *Ammonia becarii* | 310 | 52 | -0.94 | 0.010 | -2.46 | 0.012 |
| PB-5-55 | *Ammonia becarii* | 300 | 15 | 1.14 | 0.085 | -2.46 | 0.037 |
| M-17-7 | *Ammonia becarii* | 300 | 11 | 1.09 | 0.034 | -2.66 | 0.169 |
| M-17-10 | *Ammonia becarii* | 320 | 33 | 0.51 | 0.118 | -0.99 | 0.003 |
| M-17-12 | *Ammonia becarii* | 330 | 23 | 0.91 | 0.046 | -2.09 | 0.534 |
| M-17-21 | *Ammonia becarii* | 310 | 35 | 0.47 | 0.271 | -1.91 | 0.040 |
| PB-5-2 | *Aurila mehesi* | 300 | 5 | -2.86 | 0.127 | -0.58 | 0.170 |
| PB-5-3 | *Aurila notata* | 300 | 5 | -5.13 | 0.741 | -0.68 | 0.274 |
| PB-5-9 | *Aurila notata* | 280 | 3 | -6.01 | 0.327 | -0.22 | 0.039 |
| PB-5-10 | *Aurila notata* | 310 | 9 | -6.11 | 0.090 | -0.53 | 0.102 |
| PB-5-12 | *Aurila notata* | 300 | 8 | -3.29 | 0.156 | -1.48 | 0.106 |
| PB-5-15 | *Aurila notata* | 300 | 9 | -4.87 | 0.296 | -0.56 | 0.260 |
| PB-5-18 | *Aurila mehesi* | 300 | 10 | -4.24 | 0.293 | -1.14 | 0.228 |
| PB-5-19 | *Aurila mehesi* | 310 | 8 | -2.76 | 0.323 | -2.65 | 0.306 |
| PB-5-22 | *Aurila mehesi* | 320 | 7 | -2.45 | 0.085 | -1.81 | 0.031 |
| PB-5-24 | *Aurila mehesi* | 310 | 4 | -0.50 | 0.009 | -2.23 | 0.236 |
| PB-5-27 | *Aurila mehesi* | 330 | 6 | -2.37 | 0.388 | -2.21 | 0.174 |
| PB-5-30 | *Aurila mehesi* | 300 | 7 | -2.23 | 0.217 | -2.63 | 0.006 |

ctnd. **TAB. 4.**

| | | | | | | | |
|---|---|---|---|---|---|---|---|
| PB-5-32 | *Aurila mehesi* | 300 | 11 | -1.93 | 0.113 | -0.89 | 0.161 |
| PB-5-35 | *Aurila notata* | 300 | 9 | -1.79 | 0.113 | -2.58 | 0.154 |
| PB-5-39 | *Aurila notata* | 310 | 14 | -5.21 | 0.073 | -1.44 | 0.426 |
| PB-5-40 | *Aurila notata* | 300 | 8 | -4.36 | 0.028 | -0.70 | 0.528 |
| PB-5-41 | *Aurila notata* | 320 | 9 | -3.84 | 0.053 | -1.42 | 0.152 |
| PB-5-52 | *Aurila notata* | 310 | 8 | -3.57 | 0.180 | -1.52 | 0.237 |
| PB-5-56 | *Aurila notata* | 320 | 9 | -3.39 | 0.439 | -2.44 | 0.152 |
| M-17-1 | *Aurila mehesi* | 290 | 10 | -2.75 | 0.285 | -1.82 | 0.031 |
| M-17-3 | *Aurila mehesi* | 330 | 8 | -2.65 | 0.082 | -2.23 | 0.220 |
| M-17-5 | *Aurila mehesi* | 320 | 8 | -2.96 | 0.227 | -1.27 | 0.304 |
| M-17-9 | *Aurila mehesi* | 300 | 16 | -2.91 | 0.300 | -0.85 | 0.181 |
| M-17-15 | *Aurila notata* | 290 | 14 | -1.71 | 0.014 | -1.79 | 0.127 |
| M-17-17 | *Aurila notata* | 300 | 4 | -4.97 | 0.447 | -0.40 | 0.009 |
| M-17-19 | *Aurila notata* | 300 | 4 | -4.11 | 0.308 | -0.43 | 0.004 |
| M-17-23 | *Aurila notata* | 300 | 9 | -5.03 | 0.020 | -0.57 | 0.169 |
| M-17-27 | *Aurila notata* | 310 | 8 | -3.55 | 0.356 | -1.45 | 0.083 |
| M-17-28 | *Aurila notata* | 300 | 15 | -3.38 | 0.040 | -2.11 | 0.295 |
| M-17-33 | *Aurila notata* | 320 | 17 | -4.20 | 0.428 | -1.81 | 0.100 |
| M-17-39 | *Aurila notata* | 320 | 6 | -3.61 | 0.221 | -2.31 | 0.314 |
| M-17-41 | *Aurila notata* | 330 | 9 | -3.14 | 0.164 | -2.70 | 0.070 |
| M-17-43 | *Aurila notata* | 310 | 12 | -4.20 | 0.099 | -1.25 | 0.012 |
| M-17-45 | *Aurila notata* | 300 | 10 | -3.19 | 0.849 | -2.03 | 0.203 |

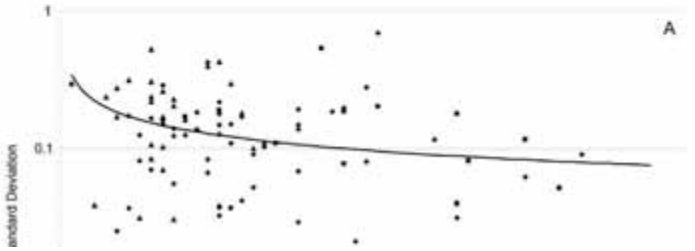


**Figure 7:** Variations in standard deviations of carbon and oxygen isotope measurements as a function of the number of individuals considering all three genera of foraminifera and ostracods from various levels in Sarmatian boreholes of Hungary (Fig. 2).

The quality of the fit being so weak when considering all three genera from various sample levels simultaneously (due to inter-sample and between-taxon isotopic differences), this approach was restricted to a taxonomically homogeneous pool of *Elphidium* foraminifera extracted from the same, *Elphidium*-rich sample level from the Mány-17 borehole (Fig. 2), from which sub-samples composed of 5, 10, 20, 30 and 40 individual shells (corresponding to samples from 50 to 900 μg) were generated by randomly picking-up the fossils under a stereomicroscope. Single-cell samples were not considered here due to their very small weight (average individual shell weight: 16.5 ± 3.8 μg), involving relatively high associated instrumental uncertainty when compared to the 5 to 40-cell samples, and thus biasing upward the estimate of inter-biological sample variability effects. For each sub-sample size, four distinct sub-samples have been made, allowing the computation of a between-biological sample standard deviation (Table 5). Figure 8 shows that this standard deviation increases with the number of individuals decreasing according to the following power laws (including an additive constant which corresponds to the background instrumental standard deviation – a value reached asymptotically when analyzing an "infinite" pool of individuals):

$$\text{SD of } \delta^{18}O = 0.133 + 34.268\, N^{-2.485},\ R^2 = 0.83\ (p = 8.9 \cdot 10^{-2})$$

$$\text{SD of } \delta^{13}C = 0.057 + 2.748\, N^{-0.829},\ R^2 = 0.92\ (p = 9.8 \cdot 10^{-3}),$$

where $N$ is the number of individuals in the sample. According to the prediction confidence interval belts associated to these equations, there is a probability of 95% (lower bound of the 90% C.I. belt) to obtain between-biological sample standard deviations higher than 1.02‰ and 1.45‰ for different $\delta^{18}O$ and $\delta^{13}C$ measurements of single specimens of *Elphidium*, respectively. Such predicted inter-individual variability is about one order of magnitude higher than the background instrumental

uncertainty, indicating that a significant amount of variability of eco-physiological origin is added when considering biological organisms such as foraminifera.

**TABLE 5:** Variations in carbon and oxygen isotope compositions of randomly generated sub–samples of Sarmatian *Elphidium* from a homogeneous pool of *Elphidium macellum* foraminifera extracted from the same level of Mány-17 borehole, Hungary as reported in Figure 2.

| Sample # | Individuals (n) | Weight (µg) | $\delta^{13}C$ ‰ V–PDB | $\delta^{18}O$ ‰ V–PDB |
|---|---|---|---|---|
| Elphi M17_1 | 5 | 60 | 0.18 | -2.11 |
| Elphi M17_2 | 5 | 50 | -0.66 | -1.52 |
| Elphi M17_3 | 5 | 50 | -0.55 | -1.93 |
| Elphi M17_4 | 5 | 60 | -1.72 | -2.83 |
| Elphi M17_5 | 10 | 130 | 0.33 | -1.43 |
| Elphi M17_6 | 10 | 140 | -0.62 | -1.75 |
| Elphi M17_7 | 10 | 140 | -0.21 | -1.63 |
| Elphi M17_8 | 10 | 160 | -0.26 | -1.66 |
| Elphi M17_9 | 20 | 380 | 0.30 | -1.69 |
| Elphi M17_10 | 20 | 330 | 0.02 | -1.43 |
| Elphi M17_11 | 20 | 350 | -0.50 | -1.68 |
| Elphi M17_12 | 20 | 330 | -0.15 | -1.88 |
| Elphi M17_13 | 30 | 570 | -0.11 | -1.43 |
| Elphi M17_14 | 30 | 540 | 0.27 | -1.55 |
| Elphi M17_15 | 30 | 610 | -0.12 | -1.79 |
| Elphi M17_16 | 30 | 610 | -0.33 | -1.61 |
| Elphi M17_17 | 40 | 710 | -0.26 | -1.47 |
| Elphi M17_18 | 40 | 850 | -0.34 | -1.64 |
| Elphi M17_19 | 40 | 790 | -0.51 | -1.74 |
| Elphi M17_20 | 40 | 900 | -0.13 | -1.73 |

**Figure 8:** Variations in standard deviations of carbon and oxygen isotope measurements as a function of the number of individuals from the same pool of *Elphidium* foraminifera from the Mány-17 borehole (Fig. 2).

# 4. DISCUSSION

Isotopic studies of carbonated skeletons cannot escape the question of a possible diagenetic alteration that may potentially modify their pristine compositions. Selected foraminifera and ostracod samples from the Miocene deposits of Hungary have been already evaluated for their state of preservation as attested by the quality of their ultrastructure imaged by SEM techniques (Tóth et al., 2010). However, no definitive criterion is available in order to discard unambiguously alteration processes responsible for sizable changes in the post-depositional compositions of carbonated fossils. Nevertheless, on the basis of mass balance considerations, one can expect two isotopic patterns of water–mineral interactions that could operate within sedimentary deposits. The first one is the production of homogenized isotopic compositions of fossils in response to large volumes of aqueous fluids interacting with the hosting sediment; the second one, driven by low water–mineral ratios, should produce isotopic heterogeneities without any relation to the sample size (i.e., number of sampled individuals). These two scenarios do not match the observed distribution of isotopic compositions in studied foraminifera and ostracod shells.

Carbon and oxygen isotope compositions of the studied carbonated fossil shells show unambiguously that empirical between-biological sample variability associated with $\delta^{18}O$ and $\delta^{13}C$ largely exceeds the background instrumental uncertainty and clearly relates to inter-individual variability (Fig. 7 and 8). This result clearly impacts interpretation of variations in both $\delta^{18}O$ and $\delta^{13}C$ values of marine carbonated microfossils as indicators of change in ambient seawater temperature and productivity.

Indeed, in order to be able to detect subtle variations in seawater temperature based on $\delta^{18}O$ values, a minimum of 35 pooled specimens of *Elphidium* is necessary to reach a between-sample standard deviation $\leq 0.25‰$ with a probability of 95%, corresponding to an estimated temperature uncertainty $\leq \pm 1°C$ at a 95% confidence level (Fig. 8). The analysis of less than 3 pooled individual shells returns standard deviation values $\geq 0.25‰$ in more than 95% of the sample cases, a value exceeding 1‰ (corresponding to an actual seawater estimated temperature uncertainty of at least ±4°C at a 95% confidence level) when a single specimen of *Elphidium* is analyzed. In such cases of large uncertainty, the detection of thermal events such as changes in oceanic circulation or climatic events recorded by coastal waters (whose amplitudes rarely exceed 5°C as documented since the Mesozoic; Shackleton, 1986; Norris and Röhl, 1999; Lécuyer et al., 2003; Pucéat et al., 2003; Joachimski et al., 2009) obviously becomes problematic, if not impossible. The oxygen isotope composition of benthic foraminifera such as *Elphidium* has been also extensively used as a proxy of variations in the $\delta^{18}O$ of seawater as a consequence of changes in the continental ice volume. Once again, this threshold of ~1‰ associated with the analysis of a single foraminifera shell constitutes a “biological isotopic noise” in the same order of magnitude as the variation in the $\delta^{18}O$ of the oceans resulting from ice cap growth during a glacial stage or a complete melting of existing ice caps during

a greenhouse interlude (Shackleton and Kennett, 1975; Billups and Schrag, 2003; Pekar and DeConto, 2006. Again, these results challenge the interpretation of the $\delta^{18}O$ signal for coastal benthic foraminifera only. For the open ocean record, including benthic and planktonic isotopic compositions on a regional interval, quantitative estimations based on several specimens seem to stay valid, taking into account local perturbations such as current strength or origin (Van Sebille et al., 2015). In addition to this study, the same approach needs to be performed on individual benthic or planktonic specimen taken in large scale areas, to investigate open-ocean parameter reconstructions. Deeper studies could also test differences observed at several depths in the water column, taking into account different sizes within a single foraminifera species.

Concerning carbon isotope measurements, a minimum of 15 and 44 *Elphidium* individuals is required in order to reach between-sample standard deviations ≤ 0.5‰ and ≤ 0.25‰, respectively (Fig. 8). The carbon isotope analysis of a single specimen generates a standard deviation ≥ 1.45‰ in 95% of the sample cases; such threshold is comparable to secular changes in the $\delta^{13}C$ values recorded in the marine carbonate deposits which are interpreted either as variations in the primary production at time scales of about 50,000 yr, or variations in the burial or oxidation rates of sedimentary organic matter at time scales of about 1 Myr (e.g. Magaritz et al., 1992; Kump and Arthur, 1999). However, this between-sample standard deviation predicted for a single specimen analysis in a homogeneous taxonomical and environmental/climatic context is significantly lower than some spectacular carbon isotope excursions recorded in sediments and which were interpreted as related to extreme events such as food chain rupture, volcanic paroxysm and large methane release by clathrates (e.g. Röhl et al., 2000; Pálfy et al., 2001; Hesselbo et al., 2002).

Contrasting with the two relations inferred for $\delta^{18}O$ and $\delta^{13}C$, it is worth noting that the average observed values of inter-biological sample standard deviation in the 5–40 specimens and 50–900 μg sample weight ranges are slightly higher for $\delta^{13}C$ than for $\delta^{18}O$ measurements. Actually, based on the instrumental standard deviations as evidenced above, one should expect the reverse situation if such inter-biological sample standard deviations were the consequence of an instrumental mass fractionation (the average instrumental error is ~2.3 times larger for $\delta^{18}O$ than for $\delta^{13}C$ based on 29 Carrara marble aliquots). Indeed, such result clearly points to the fact that the inter-biological sample variability evidenced here does originate in an inter-individual natural heterogeneity (i.e., biological variability) rather than in an instrumental fractionation spurious analytical effect. This result makes sense with regard to the specific environmental life style of *Elphidium*, a coastal species for which strong natural variations in salinity and temperature could be expected.

Inter-individual $\delta^{18}O$ and $\delta^{13}C$ variations as evidenced here between specimens from the same foraminifera genus and fossil level are most likely resulting from eco-physiological intrinsic differences in metabolism (e.g., individual position within the autotrophy-heterotrophy gradient) and environmental conditions (e.g., depth-related changes in temperature and luminosity, and composition of dissolved inorganic carbon). In addition, such irreducible biological variability could be strongly, but

artefactually enhanced by cryptic biological speciation events as increasingly evidenced in marine, planktic as well as benthic organisms (Knowlton, 1993; de Vargas et al., 1999, 2004; Irigoien et al., 2004; Chen and Hare, 2008; Darling and Wade, 2008). An efficient way to further exploring such possibility should be to independently perform the kind of analysis leading to Figure 8 on distinct morphological species showing contrasted cryptic diversity contexts (the higher the cryptic diversity, the steeper the decreasing slope of the number of individuals *vs*. between-sample standard deviation relation). The ongoing effort in developing morphometrical recognition models of cryptic species (e.g., Morard et al. 2009) should allow solving this problem in the future. Future studies could also investigate open ocean foraminifera species, benthic or planktonic, usually used for large-scale (in both space and time) paleoceanographic reconstructions.

## 5. CONCLUSION

We have shown in this study that recent automated systems designed for the analyses of $\delta^{13}C$ and $\delta^{18}O$ from carbonate samples are capable of measuring reliably small quantities of pure calcite down to 5–10 μg with instrumental standard deviations close to 0.1‰. Such analytical accuracy opens up possibilities for the analysis of small microfossils like foraminifera, especially for paleoclimate reconstruction purposes. Nevertheless, data generated from small numbers of specimens (e.g., carbonated shells from single-cell organisms) have to be considered with great caution. Indeed, our results show a general trend to increase the between-biological sample standard deviation for both $^{13}C$ and $^{18}O$ measurements when decreasing the number of specimen analysed. Based on a systematic study performed on a homogeneous pool of *Elphidium* coastal benthic foraminifera, we estimate that there is a probability of 95% to obtain between-biological sample standard deviations higher than 1.02‰ and 1.45‰ for $\delta^{18}O$ and $\delta^{13}C$ measurements of various single shells, respectively.

Such biological intrinsic and irreducible variability observed between coeval samples clearly questions the interest for single-cell analyses for environments undertaking rapid and strong variations in their physical parameters, such as salinity and temperature. For this specific example, paleotemperature estimates should not be done on single foraminifera $\delta^{18}O$ measurements.

## REFERENCES

1. Bauch H.A., Erlenkeuser H., Bauch D., Mueller-Lupp T., Taldenkova E., 2004. Stable oxygen and carbon isotopes in modern benthic foraminifera from the Laptev Sea shelf: implications for reconstructing proglacial and profluvial environments in the Arctic. Mar. Micropal. 5, 285–300.

2. Billups K., Schrag D.P., 2003. Paleotemperatures and ice volume of the past 27 Myr revisited with paired Mg/Ca and $^{18}O/^{16}O$ measurements on benthic foraminifera. Paleoceanography 17(1), 1003, doi: 10.1029/2000PA000567.
3. Billups K., Spero H.J., 1995. Relationship between shell size, thickness and stable isotopes in individual planktonic foraminífera from two equatorial Atlantic cores. J. Foram. Res. 25, 24–37.
4. Chen G., Hare M.P., 2008. Cryptic ecological diversification of a planktonic estuarine copepod, *Acartia tonsa*. Molecul. Ecol. 17, 1451–1468.
5. Darling K.F., Wade C.M., 2008. The genetic diversity of planktic foraminifera and the global distribution of ribosomal RNA genotypes. Mar. Micropal. 67, 216–238.
6. Epstein S., Buchsbaum R., Lowenstam H.A., Urey, H.C., 1953. Revised carbonate–water isotopic temperature scale. Geol. Soc. Am. Bull. 64, 1315–1326.
7. Fink C., Baumann K.-H., Groeneveld J., Steinke S., 2010. Strontium/Calcium ratio, carbon and oxygen stable isotopes in coccolith carbonate from different grain-size fractions in South Atlantic surface sediments. Geobios 43, 151–164.
8. Görög A., 1992. Sarmatian foraminifera of the Zsámbék Basin, Hungary. Annales Universitatis Scientiarum Budapestinensis, Sectio Geologica 29, 31–153.
9. Hesselbo S.P., Robinson S.A., Surlyk F., Piasecki S., 2002. Terrestrial and marine extinction at the Triassic-Jurassic boundary synchronized with major carbon-cycle perturbation: A link to initiation of massive volcanism? Geology 30, 251–254.
10. Holmes J.A., 1996. Trace-element and stable-isotope geochemistry of non-marine ostracod shells in Quaternary palaeoenvironmental reconstruction. J. Paleolimnol. 15, 223–235.
11. Huber B.T., Norris R.D., Macleod K.G., 2002. Deep-sea paleotemperature record of extreme warmth during the Cretaceous. Geology 30, 123–126.
12. Huber B.T., Hodell D.A., Hamilton C.P., 1995. Mid- to Late Cretaceous climate of the southern high latitudes: stable isotopic evidence for minimal equator-to-pole thermal gradients. Geol. Soc. Am. Bull. 107, 1164–1191.
13. Irigoien X., Huisman J., Harris R.P., 2004. Global biodiversity patterns of marine phytoplankton and zooplankton. Nature 429, 863–867.
14. Jenkyns H.C., Forster A., Schouten S., Damsté J.S.S., 2004. High temperatures in the Late Cretaceous Artic Ocean. Nature 432, 888–892.
15. Joachimski M.M., Breisig S., Buggisch W., Talent J.A., Mawson R., Gereke M., Morrow J.M., Day J., Weddige K., 2009. Devonian climate and reef evolution: insights from oxygen isotopes in apatite. Earth. Planet. Sci. Lett. 284, 599–609.
16. Kelly D.C., Bralower T.J., Zachos J.C., Silva I.P., Thomas E., 1996. Rapid diversification of planktonic foraminífera in the tropical Pacific (ODP site 865) during the Late Paleocene thermal maximum. Geology 24, 423–4126.
17. Knowlton N., 1993. Sibling species in the sea. Ann. Rev. Ecol. Syst. 24, 189–216.
18. Kump L.R., Arthur M.A., 1999. Interpreting carbon-isotope excursions: carbonates and organic matter. Chem. Geol. 161, 181–198.
19. Lea D.W., Pak D.K., Belanger C.L., Spero H.J., Hall M.A., Shackleton N.J., 2006. Paleoclimate history of Galapagos surface waters over the last 135,000 yr. Quat. Sci. Rev. 25, 1152–1167.
20. Lécuyer C., Picard S., Garcia J.-P., Sheppard S.M.F., Grandjean P., Dromart G., 2003. Thermal evolution of Tethyan surface waters during the Midle-Late Jurassic: Evidence from $\delta^{18}O$ values of marine fish teeth. Paleoceanography 18 (3), 1076, doi:10.1029/2002PA000863.

21. Magaritz M., Krishnamurthy R.V., Holser W.T., 1992. Parallel trends in organic and inorganic carbon isotopes across the Permian/Triassic boundary. Am. J. Sci. 292, 727–739.
22. McCrea J.M., 1950. On the isotopic chemistry of carbonates and a paleotemperature scale. J. Chem. Phys. 18, 849–857.
23. Morard R., Quillévéré F., Escarguel G., Ujiie Y., de Garidel-Thoron T., Norris R.D., de Vargas C. 2009. Morphological recognition of cryptic species in the planktonic foraminifer *Orbulina universa*. Mar. Micropal. 71, 148–165.
24. Norris R.D., Röhl U., 1999. Carbon cycling and chronology of climate warming during the Palaeocene/Eocene transition, Nature 401, 775–778.
25. Pálfy J., Demény A., Haas J., Hetényi M., Orchard M., Veto I., 2001. Carbon isotope anomaly and other geochemical changes at the Triassic-Jurassic boundary from a marine section in Hungary. Geology 29, 1047–1050.
26. Pekar S.F., DeConto R.M., 2006. High-resolution ice-volume estimates for the early Miocene: Evidence for a dynamic ice sheet in Antarctica. Palaeogeogr. Palaeoclimatol. Palaeoecol. 231, 101–109.
27. Price G.D., Sellwood B.W., Corfield R.M., Clarke L., Cartlidge J.E., 1998. Isotopic evidence for palaeotemperatures and depth stratification of Middle Cretaceous planktonic foraminífera from the Pacific Ocean. Geol. Mag. 135, 183–191.
28. Pucéat E., Lécuyer C., Sheppard S.M.F., Dromart G., Reboulet S., Grandjean P., 2003. Thermal evolution of Cretaceous Tethyan marine waters inferred from oxygen isotope composition of fish tooth enamels. Paleoceanography 18 (2), 1029, doi:10.1029/2002PA000823.
29. Röhl U., Bralower T.J., Norris R.D., Wefer G., 2000. New chronology for the late Paleocene thermal maximum and its environmental implications. Geology 28, 927–930.
30. Roth P.H., 1989. Ocean circulation and calcareous nannoplankton evolution during the Jurassic and Cretaceous. Palaeogeogr. Palaeoclimatol. Palaeoecol. 74, 111– 126.
31. Saraswati P.K., 2004. Ontogenetic isotopic variation in foraminífera – Implications for palaeo prox. Current Science 86, 858–860.
32. Schidlowski M., 1987. Application of stable isotopes to early biochemical evolution on Earth. Annu. Rev. Earth. Planet. Sci. 15: 47–72.
33. Schmidt G.A., Mysak L.A., 1996. Can increased poleward oceanic heat flux explain the warm Cretaceous climate? Paleoceanography 11, 579–593.
34. Shackleton N.J., Opdyke N.D., 1973. Oxygen isotope and paleomagnetic stratigraphy of equatorial Pacific core V28-2389: oxygen isotopes temperatures and ice volumes on a $10^5$ and $10^6$ year scale. Quat. Res. 3, 39–55.
35. Shackleton N.J., 1967. Oxygen isotope analyses and Pleistocene temperatures reassessed. Nature 215, 15–17.
36. Shackleton N.J., 1986. Paleogene stable isotope events. Palaeogeogr. Palaeoclimatol. Palaeoecolol. 57, 91–102.
37. Shackleton N.J., Imbrie J, Hall M.A., 1983. Oxygen and carbon isotope record of East Pacific core V19-30: Implications for the formation of deep water in the late Pleistocene North Atlantic. Earth Planet. Sci. Lett. 65, 233–244.
38. Shackleton N.J., 1986. Paleogene stable isotope events. Palaeogeogr. Palaeoclimatol. Palaeoecolol. 57, 91–102.
39. Shackleton N.J., Kennett J.P., 1975. Paleotemperature history of the Cenozoic and initiation of Antarctic glaciation: oxygen and carbon isotopic analyses in DSDP Sites 277, 279, and 281. Init. Rep. Deep Sea Drill. Proj. 29, 743–755.

40. Shuxi C., Shackleton N.L., 1990. New technique for study on isotopic fractionation between sea water and foraminiferal growing processes. Chin. J. Ocean. Limnol. 8, 299–305.
41. Stoll H.M., Shimizu N., 2009. Micropicking of nannofossils in preparation for analysis by secondary ion mass spectrometry. Nature Protocol 4, 1038–1043.
42. Stoll H.M., Ziveri P., 2002. Separation of monospecific and restricted coccolith assemblages from sediments using differential settling velocity. Mar. Micropal. 46, 209–221.
43. Tóth E., 2008. Sarmatian (Middle Miocene) ostracod fauna from the Zsámbék Basin, Hungary. Geol. Pann. 36, 101–51.
44. Tóth E., Görög A., Lécuyer C., Moissette P., Balter V., Monostori M., 2010. Palaeoenvironmental reconstruction of the Sarmatian (Middle Miocene) Central Paratethys based on palaeontological and geochemical analyses of foraminifera, ostracods, gastropods and rodents. Geol. Mag. 147, 299–314.
45. Urey H.C., 1947. The thermodynamic properties of isotopic substances. J. Chem. Soc. London 1947, 562–587.
46. Van Sebille E., Scussolini P., Durgadoo J.V., Peeters F.J.C., Biastoch A., Weijer W., Turney C., Paris C.B. and Zahn R., 2014. Ocean currents generate large footprints in marine palaeoclimate proxies. Nature Com., doi: 10.1038/ncomms7521.
47. Vargas (de) C., Norris R., Zaninetti L., Gibb S.W., Pawlowski J., 1999. Molecular evidence of cryptic speciation in planktonic foraminifers and their relation to oceanic provinces. Proc. Nat. Acad. Sci. U.S. 96, 2864–2868.
48. Vargas (de) C., Sáez A.G., Medlin L.K., Thierstein H.R., 2004. Superspecies in the calcareous plankton. In: Thierstein, H.R., Young, J. (eds.), Coccolithophores – from Molecular Processes to Global Impact. Springer-Verlag, Heidelberg, Germany, pp. 271–298.
49. Zachos J.C., Bohaty S.M., John C.M., McCarren H., Kelly D.C., Nielsen T., 2007. The Palaeocene–Eocene carbon isotope excursion: constraints from individual shell planktonic foraminifer records. Phil. Trans. R. Soc. 365, 1829–1842.
50. Zachos J.C., Pagani M., Sloan L., Thomas E., Billups K. 2001. Trends, rhythms, and aberrations in global climate 65 Ma to Present. Science 292, 686–693.
51. Zachos J.C., Wara M.W., Bohaty S.M., Delaney M.L., Rose-Petrizzo M., Brill A., Bralower T.J., Premoli-Silva I., 2003. A transient rise in tropical sea surface temperature during the Paleocene-Eocene Thermal Maximum. Science 302, 1551–1554.